

MAPPING THE GALACTIC HALO WITH BLUE HORIZONTAL BRANCH STARS FROM THE 2DF QUASAR REDSHIFT SURVEY

ROBERTO DE PROPRIS¹, CRAIG D. HARRISON¹ PETER J. MARES²

ABSTRACT

We use 666 blue horizontal branch (BHB) stars from the 2Qz redshift survey to map the Galactic halo in four dimensions (position, distance and velocity). We find that the halo extends to at least 100 kpc in Galactocentric distance, and obeys a single power-law density profile of index ~ -2.5 in two different directions separated by about 150° on the sky. This suggests that the halo is spherical. Our map shows no large kinematically coherent structures (streams, clouds or plumes) and appears homogeneous. However, we find that at least 20% of the stars in the halo reside in substructures and that these substructures are dynamically young. The velocity dispersion profile of the halo appears to increase towards large radii while the stellar velocity distribution is non Gaussian beyond 60 kpc. We argue that the outer halo consists of a multitude of low luminosity overlapping tidal streams from recently accreted objects.

Subject headings: Galaxy: formation — Galaxy: halo — stars: horizontal-branch

1. INTRODUCTION

The motion of old stars preserves the fossil record of the earliest phases of formation in the Milky Way, as was realized in the two seminal papers by Eggen, Lynden-Bell & Sandage (1962) and Searle & Zinn (1978). The picture that has since emerged is one where the Galaxy has been built via a series of accretions and mergers (e.g., Freeman & Bland-Hawthorn 2002), in agreement with hierarchical structure formation scenarios (Johnston et al. 2008; Cooper et al. 2009). Consistent with these theoretical expectations, the halo is thickly populated by debris from past and on-going accretion events (e.g., Ibata, Gilmore & Irwin 1994; Belokurov et al. 2006). Prominent debris features have also been observed in the halos of M31 (Ibata et al. 2001, 2007; McConnachie et al. 2009), M33 (Ibata et al. 2007; McConnachie et al. 2009) and in other nearby spirals (Martinez-Delgado et al. 2010).

At the same time, the inner halo (at galactocentric distance $R_{GC} < 20$ kpc) of the Milky Way contains an old, dynamically smooth and metal-poor component, which was probably formed by rapid early merging or violent relaxation (Carollo et al. 2007, 2009; Bell et al. 2008). While the buildup of most of the inner halo is believed to take place rapidly, the outer regions of the Milky Way should grow more slowly via the disruption of dwarf galaxies: the outer halo is therefore expected to be quite inhomogeneous and dominated by large streams, clouds and plumes from infalling objects (Johnston et al. 2008; Cooper et al. 2009). The main question we need to address is the relative role of mergers and accretion vs. *in situ* formation, i.e., whether the observed structures represent the main mechanism by which the Galaxy was formed or are only a comparatively minor contribution over an ancient stellar component.

In order to clarify these issues we explore the space distribution and kinematics of the outer halo using Blue Horizontal Branch (BHB) stars. These objects have often been used as tracers of the Milky Way halo (e.g., Yanny et al. 2000; Xue et al. 2008; Brown et al. 2010). BHB stars are comparatively bright and reliable standard candles, are more common than other commonly used probes (such as Carbon stars or RR

Lyrae) and are representative of the *old* and *metal poor* stellar population that constitutes the Galactic halo. These stars can be easily identified spectroscopically, even at comparatively moderate resolution, but are sufficiently rare that extensive radial velocity surveys are needed to obtain a significant sample (Yanny et al. 2000; Xue et al. 2008; Brown et al. 2010).

Here we exploit a large suite of archival spectroscopy from the 2dF Quasar Redshift Survey (2Qz – Croom et al. 2004) to identify a sample of 666 BHB stars in the halo out to 100 kpc and explore its structure and kinematics. We use this dataset to set limits to the size of the Milky Way halo, its shape, presence of streams, degree of substructure and the velocity dispersion profile out to large radii. The next section describes the 2Qz survey and how we identified BHB stars. Section 3 discusses the 4D map of the Galactic halo we produce from these data. Section 4 examines the question of substructure in the halo and the final section analyzes the halo kinematics and discusses the results in the context of galaxy formation models, especially as apply to the Milky Way.

2. THE 2QZ DATA: IDENTIFICATION OF BHB STARS

The data for this project come from archival observations of the 2Qz survey. The 2Qz obtained spectra for $\sim 50,000$ A-colored point sources with $15 < b_J < 20.9$ selected from SuperCosmos survey photometry (Hambly et al. 2001). The targets lie in two $75^\circ \times 5^\circ$ strips on the sky, one on the celestial equator between $09^h 30^m < RA < 14^h 30^m$ and $-2.5^\circ < \delta < +2.5^\circ$ and the other centred in the Southern Galactic Cap between $22^h 00^m < RA < 03^h 00^m$ and $-32.5^\circ < \delta < -27.5^\circ$. We refer to these as the Northern and Southern samples, respectively.

The targets were selected on the basis of their u , b_J and r_F colors (photographic photometry from the SuperCosmos survey – Hambly et al. 2001) to lie in the parameter space covered by known quasars (see Croom et al. 2004 for further details): targets were selected to have $b_J < 20.9$ and $-2.5 \leq u - b_J \leq 1.5$ and $-1.5 \leq b_J - r_F \leq 2.5$, excluding a box with colors $0.4 \leq u - b_J \leq 1.5$ and $0 \leq b_J - r_F \leq 2.5$ which contains main sequence stars. Spectroscopy for these objects was obtained during 1998-2003 with the Anglo-Australian 3.9m Telescope in Coonabarabran, NSW, Australia, using the 2 degree field (2dF) multi-object spectrograph (Lewis et al. 2002). The spectra cover the entire optical range ($3500 < \lambda < 7500$

¹ Cerro Tololo Inter-American Observatory, La Serena, Chile

² Department of Astronomy, Cornell University, Ithaca, NY, USA

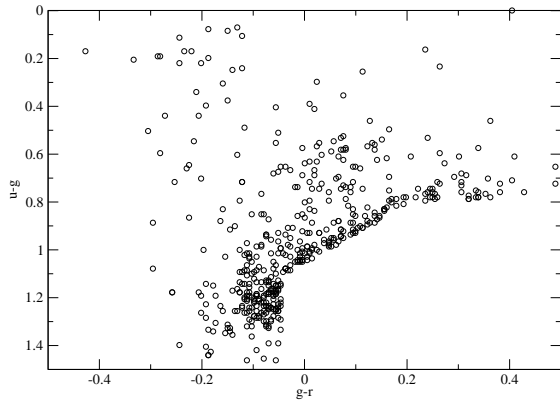


FIG. 1.— The color distribution of BHB stars identified in the 2Qz survey. The original Supercosmos colors have been transformed to the SDSS using stars in common between the two surveys.

Å) at a resolution of about 2000, with exposure times of at least one hour per target, although a fraction of the objects were exposed for considerably longer, if they happened to lie in a region where the 2dF tiles used by the survey overlapped (to insure greater completeness) or the field was reobserved (because of lower than expected signal).

As with all color-selected surveys, 2Qz suffers from significant contamination from QSO-colored stellar objects, such as white dwarfs, disk A stars, blue stragglers and BHB stars, although this is minimized by observing at high galactic latitude. The data were reduced and redshifted via a semi-automated technique and whenever a stellar redshift ($z = 0$) was obtained, the object was discarded from further analysis but placed in the database. We proceeded to retrieve all stellar spectra from the database and classify them on the basis of the equivalent widths of the H_γ and H_δ Balmer lines, to identify a sample of 666 *bona fide* BHB stars. Following Yanny et al. (2000); Xue et al. (2008); Brown et al. (2010) we first measured radial velocities for all star by cross correlating with synthetic templates from the library of Munari et al. (2005): the templates had temperatures and gravities typical of A-stars and field horizontal branch stars (Beers et al. 2001). We then fit Gaussian curves to the H_γ and H_δ lines and measured the width of the Gaussian fit at 20% of the normalized continuum level: this indicator $D_{0.2}$ has been shown to be a good discriminator between BHB stars, blue stragglers and other contaminants (Pier 1983; Yanny et al. 2000). We only used spectra that we deemed to be of sufficient quality to allow a secure classification. In order to be included in our sample radial velocities had to be determined to within 50 km s^{-1} and the H_γ and H_δ widths had to have errors of less than 20%. In order to classify stars as *bona fide* BHB stars we require that the mean $D_{0.2}$, from both lines, lie between 17 and 31 Å (as in Pier 1983; Yanny et al. 2000, leaving a total of 666 BHB stars in our sample.

Figure 1 shows the distribution of the stars in the $u - g$ vs. $g - r$ plane, where we transformed our Supercosmos $u - b_J$ and $b_J - r_F$ colors to the Sloan system by using stars in common in the equatorial region shared by 2Qz and the SDSS. This is at least qualitatively similar to the color distribution of stars in previous work (e.g., compare Fig. 1 in Brown et al. 2010) and suggests that our sample is comparable to those used in previous studies, in terms of selection criteria and degree of contamination from blue stragglers and other A-colored objects.

As our targets span a relatively narrow range in colors (as

selected by the 2Qz survey) we assumed an absolute magnitude of $M_{b_J} = 0.7 \pm 0.2$ which is typical for BHB stars (Layden et al. 1996). We finally used these distances, the known sky positions and the measured radial velocities to place all our stars on a cylindrical coordinate system at rest with respect to the centre of the Galaxy, assuming Solar positions as in Dehnen & Binney (1998). This yields a 4-dimensional (position, distance and radial velocity) map of the galactic halo in two widely separated (150°) lines of sight.

3. THE 4D STRUCTURE OF THE MILKY WAY HALO

In Figure 2 we plot the 4D map of the Galactic halo we produced, projected along the three most relevant dimensions. It is clear from this figure that the halo of the Milky Way extends to at least 100 kpc from the Galactic centre, and likely well beyond (the edge of the map is set by the magnitude limit of 2Qz data), in both directions we survey. This is considerably larger than previously believed and comparable to the large metal-poor halo observed in the Andromeda galaxy (Chapman et al. 2006; Kalirai et al. 2006; Koch et al. 2008); it would include several of the dwarf galaxy satellites (including the Magellanic clouds) within the Galaxy’s stellar halo. As a matter of fact the Sextans dwarf is visible in Fig. 2 at $x \sim -20$ kpc and $y \sim +50$ kpc. Such large metal-poor halos may be ubiquitous (e.g., in NGC 3379 – Harris et al. 2007) and may be a common byproduct of early galaxy formation.

In previous work, the SDSS has identified BHB stars out to 60 kpc from the Galactic centre (Xue et al. 2008), while the Hypervelocity Stars Survey (Brown et al. 2010) found a BHB star sample to a distance of 75 kpc. The Spaghetti survey (Morrison et al. 2000; Starkeburg et al. 2009) has observed halo red giants to a distance of 100 kpc, and star counts in the COSMOS field identify a halo component to a distance of 80 kpc (Robin et al. 2007). Our study reaches deeper than nearly all these and covers a larger field of view than all except the SDSS (it is comparable to the Hypervelocity Stars Survey coverage). However, we sample the BHB stars more densely as all potential targets have been targeted by the 2Qz survey, although of course we are not able to classify all stars. Since we cover nearly diametrically opposite areas on the sky, we argue that the detection of the stellar halo in our data is not due to possible diffuse structures on the sky that accidentally lie in our line of sight (as for pencil-beam studies such as COSMOS or the Spaghetti survey) and the Milky Way halo truly extends to large radii.

Figure 3 shows the radial density profile of the halo along both directions we survey. In both cases we obtain a good fit to a single power law of index $R^{-2.5 \pm 0.2}$. This is somewhat shallower than the $\sim R^{-3}$ found by Morrison et al. (2000) and predicted by theory, but is in good agreement with previous measurements using BHB stars by Xue et al. (2008) and Brown et al. (2010). We are of course incomplete in that we cannot detect and identify all BHB stars in 2Qz. This incompleteness is a complex function of our ability to reliably classify stars as a function of spectroscopic signal-to-noise. Naively, we would preferentially miss the most distant objects, that would tend to make the radial profile steeper than it actually is, while contamination from blue stragglers would tend to make the profile flatter. The similarity between our profiles and those derived by (e.g.) Yanny et al. (2000); Xue et al. (2008) and Brown et al. (2010) argues that our contamination fraction (from blue stragglers) and completeness are not too different from previous samples.

In any case, this should not affect our differential measure-

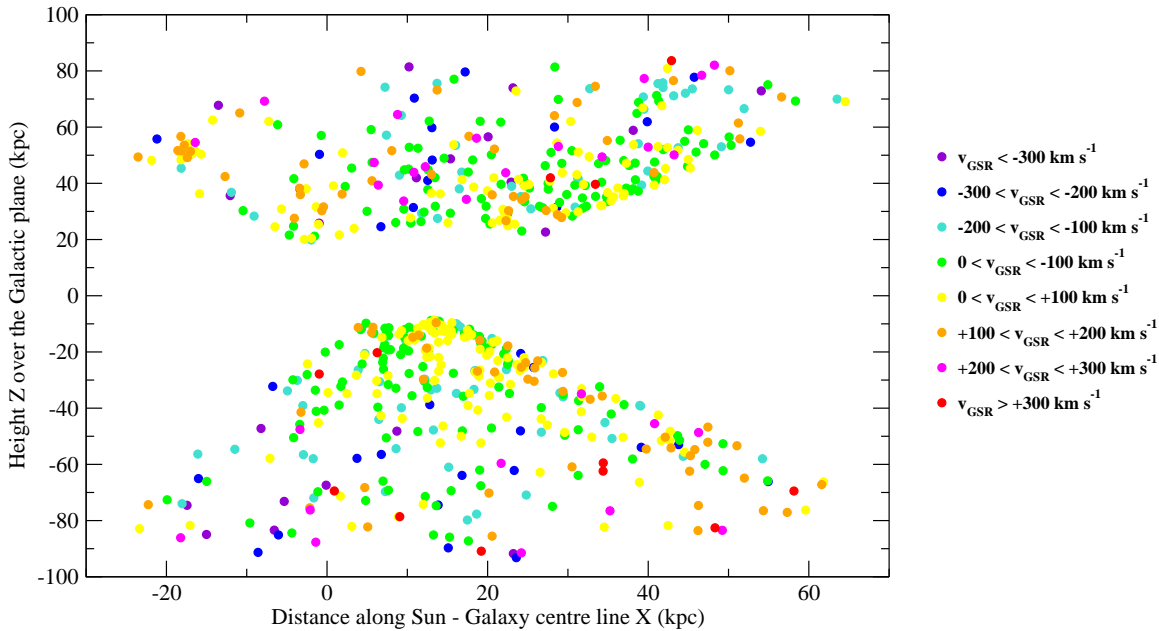


FIG. 2.— The 4D map of the Galactic halo, with stars projected on the Galactic plane (along a line connecting the Sun to the Galactic centre) on the x-axis and vs. their height above the plane on the z-axis. The stars are color-coded by their Galactocentric radial velocity, as indicated in the figure legend.

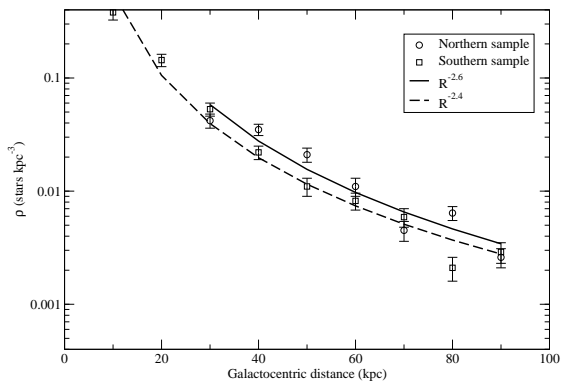


FIG. 3.— Radial density profiles for BHB stars in the halo and best power-law fits to the Northern and Southern samples separately.

ment of the radial density profile for the two individual sight-lines we survey. The similarity in the profile slope then argues that the stellar halo of the Galaxy is spherical (Majewski et al. 2003; Smith, Wyn Evans & Ahn 2009), although more sight-lines would be helpful to obtain a more precise estimate for the halo’s axial ratio.

In a recent survey of RR Lyrae in SDSS stripe 82, Watkins et al. (2009) and Sesar et al. (2010) find that the halo radial profile becomes very steep (R^{-6}) at galactocentric radii larger than 40 kpc and the the outer halo seems to be dominated by a large structure known as the Virgo-Aquila cloud, which is either an infalling dwarf galaxy or a tidal stream. However this is not observed in our data, or those of Brown et al. (2010). One possibility is that the RR Lyrae distribution is more concentrated towards the Galactic centre, as RR Lyrae tend to be more metal rich than BHB stars and the halo appears to have an abundance gradient (Carollo et al. 2007, 2009). This would create an apparent break in the radial profile, reflecting the lower overall metallicity of the sample at large distances.

4. SUBSTRUCTURE IN THE HALO

Inspection of Fig. 2 also shows that there are no obvious large kinematically coherent features, such as streams, plumes or shells, in our 4D map of the Galactic halo. We identify three possible structures: one is the Sextans dwarf, as previously mentioned. A plume of infalling stars is present in the top right-hand corner of Fig. 2 at $x \sim +40$ kpc and $y \sim +80$ kpc. This may be related to the Virgo-Aquila structure. Finally, a small clump of objects is observed in the direction of Piscis Austrinus at $x \sim +40$ kpc and $y \sim -50$ kpc and may be an undiscovered dwarf. Nevertheless, we do not appear to observe the large streams expected in simulations (Johnston et al. 2008; Cooper et al. 2009) and the outer halo appears to be more homogeneous than predicted.

We can quantify the presence of streams or otherwise using the Great Circle Stream method of Lynden-Bell & Lynden-Bell (1995) in Figure 4. We compute the excess radial energy of each star compared to a smoothed Galactic potential and compare the results to a randomized sample, where we scramble the velocities, but not the positions, of stars, 1000 times. Streams would show up in this figure as long lines of stars. It is easy to see that our sample contains no significant stellar streams. The large metal poor outer halo appears to represent an extension of the smooth metal poor inner halo structure (Carollo et al. 2007, 2009; Bell et al. 2008).

However, lack of large streams does not mean lack of substructure. Bell et al. (2008) find that about 40% of stars in the inner halo are substructured, even if the only prominent stream in their data is the well known Sagittarius stream, while Starkenburg et al. (2009) find that around 25% of the stars in the Spaghetti survey are more clustered than expected from a random distribution. We apply the 4-distance method used by Starkenburg et al. (2009) to our data in Figure 5. This is essentially a version of the correlation function for

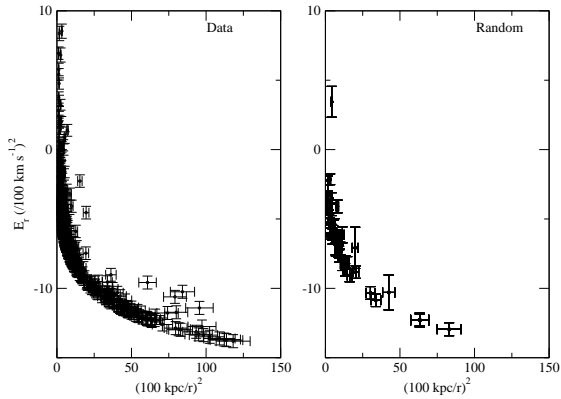


FIG. 4.— The Great Circle Stream method applied to stars in our sample. We plot the excess radial energy of each stars with respect to a smoothed Galactic potential vs. its radial distance from the centre of the Galaxy. The left hand panel shows the actual data, where the right hand panel is a randomization. No streams are observed in these figures as long lines of stars having the same excess radial energy.

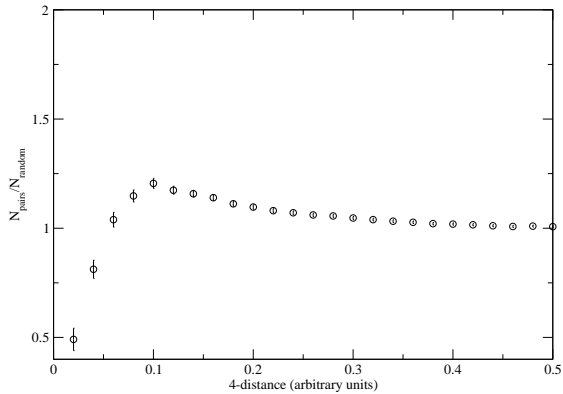


FIG. 5.— The excess fraction of stellar pairs over random (see text) in 4-dimensional distance for our sample of BHB stars.

4-dimensional data, computing the excess number of stellar pairs in position and velocity compared to a random sample (realized by scrambling the velocities but not the positions of the stars in the data) as a function of distance in 4-dimensional space. The angular, spatial and velocity separations are scaled by the range in these quantities covered by the data.

At a 5σ level we find that at least 20% of our stars are more paired than random. This agrees, broadly, with the estimates by Bell et al. (2008) for the inner halo and Starkenburg et al. (2009) for the outer halo. In addition we detect a decrease in the correlation strength at small 4-distance. This is expected if the outer halo is dynamically young and suggests the presence of numerous streamlets and a complex structure, too weak to be resolved by our data. We present further evidence to this effect from an analysis of halo kinematics.

5. KINEMATICS OF THE HALO

The kinematics of metal-poor stars in the halo yield information on the earliest phases of galaxy formation (Eggen et al. 1962) and the shape of the Galactic potential. Until recently, known samples of halo stars were small, especially at large galactocentric distances. Battaglia et al. (2005) used a heterogeneous sample of red giants, BHB stars, globular clusters and dwarf galaxies to trace the velocity disper-

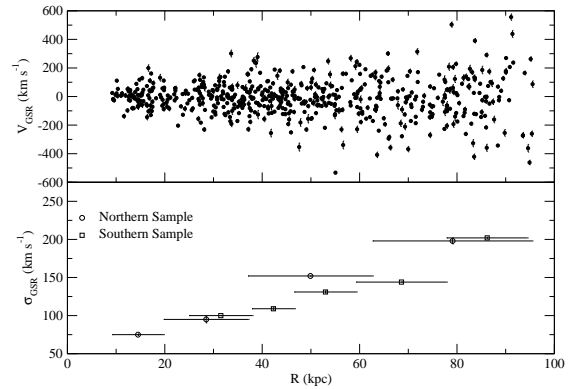


FIG. 6.— *Top panel:* Run of radial velocities of BHB stars as a function of Galactocentric distance. *Bottom panel:* The radial velocity dispersion profile of the Galactic halo in both Northern and Southern samples. Each bin contains equal numbers of stars and the velocity dispersion and its error are calculated using a maximum likelihood method. The error bars on points for the x-axis represent the size of the bin used.

sion profile of the Galaxy out to ~ 100 kpc, finding a mildly declining profile. Using BHB stars in SDSS Xue et al. (2008) found a flat or mildly declining profile out to 60 kpc and therefore inferred a large mass of the Milky Way. Brown et al. (2010) also derive a mildly declining profile out to 75 kpc using BHB stars in the Hypervelocity Star Survey. In all these cases, the fits depends strongly on the accuracy of the last (most distant) data points, which generally contain fewer objects.

We use our data to derive the velocity dispersion profile in both Northern and Southern samples separately. We use bins containing equal numbers of stars and calculate the velocity dispersion and its error following a maximum likelihood approach (Walker et al. 2006). Figure 6(a,b) plots our results. While we are in reasonable agreement with previous work over the range where we overlap, we find evidence of a rising velocity dispersion at large radii, in both fields we study. This is unlike the results of Battaglia et al. (2005) and Brown et al. (2010), although we reach farther into the distant halo than they do. In the former case, the heterogeneous sample and its relatively small size may cause part of the difference, as it is known that different tracers have different kinematics (e.g., Kinman et al. 2007). In the latter case, we and Brown et al. (2010) use the same tracers, but while our stars are concentrated in two narrow strips, Brown et al. (2010) uses a wide region selected from the SDSS. We have more stars (by a factor of about 3) than they do at large ($R > 50$ kpc) distances. One possibility is that we sample this regime more densely, especially if the halo is as inhomogeneous as theory suggests and as the evidence from Fig. 5 also argues.

Is it possible that our result may be affected by contamination from blue straggler stars. Since these objects are 2 to 3 magnitudes fainter than BHB stars, blue stragglers will contaminate the bins at $R_{GC} > 40$ kpc with objects that truly lie at distances of 10 to 30 kpc. The selection procedures we describe above should exclude most contaminants but even if we are as effective as previous studies, $\sim 20\%$ of our sample may consist of blue stragglers. In order to assess the effects of contamination, we have used a model distribution function for the velocity dispersion profile of our Galaxy from van Hese, Baes & Dejonghe (2009), with Galactic mass of $1.1 \times 10^{13} M_{\odot}$ and halo scale radius of 40.5 kpc from Dehnen & Binney (1998). We sampled 100 stars at distances of 10 to 100 kpc with a Gaussian random deviate having $\sigma(r)$ from van Hese et al.

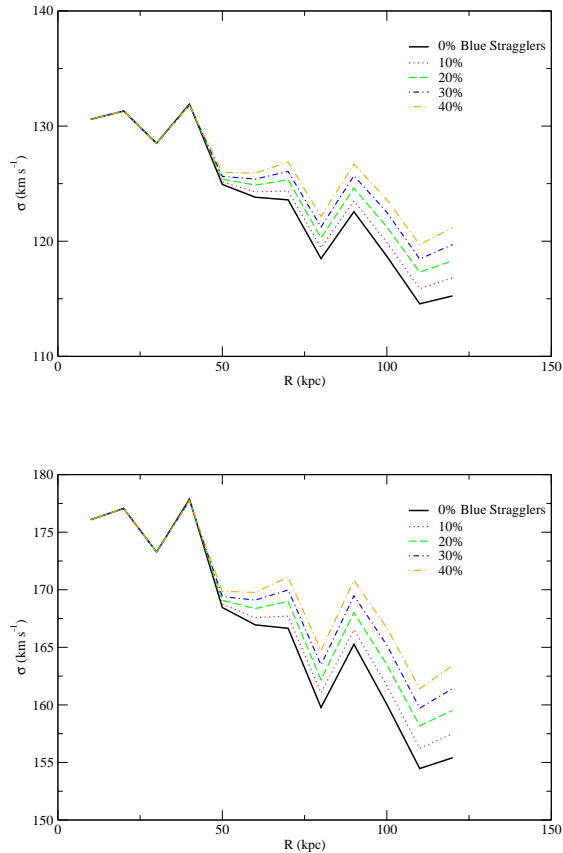


FIG. 7.— The effect of BHB star contamination on the velocity dispersion profile of the Galaxy. The top panel is for a distribution with no velocity anisotropy while the bottom panel assumes that all velocities are tangential at large radii. See text for details. The degree of contamination assumed is indicated in the legend.

(2009) and zero mean velocity. We adopted two cases: one with no velocity anisotropy $\beta_0 = \beta_{\text{inf}} = 0$ and one with fully tangential radial velocities at infinity ($\beta_0 = 0$; $\beta_{\text{inf}} = 1$). For each of these we adopted a variable contamination, between 10% and 40%, from blue straggler stars, which we assumed to be 2.5 mag. fainter than BHB stars. We replaced this fraction of stars in each bin with $R_{GC} > 40$ kpc, with blue stragglers at the appropriate distance, with velocities sampled from a Gaussian random deviate with $\sigma(r)$ from van Hese et al. (2009), at the appropriate r for a contaminating blue straggler. The results of this exercise are shown in Figure 7. Although the blue stragglers increase the measured velocity dispersion at large radii (compared with the theoretical profile), they do not produce a flat or rising velocity dispersion profile (as in the bottom panel of Fig. 6) even at 40% contamination, and even for the relatively flat $\sigma(r)$ profile produced by the fully isotropic model.

In Figure 8 we plot the histograms of radial velocities for all stars in 6 bins, containing equal numbers of objects and covering a range of distances. We see that while the distributions are acceptably Gaussian within the inner 60 kpc, we observe both an increase in dispersion and a loss of Gaussianity in the two outer bins. This is consistent with what we observe in

Fig. 5 and 6, where we find indications of an increasing velocity dispersion and a dynamically young and substructured halo. If the outer halo consists of a myriad of streamlets, accreted more or less recently from the disruption of satellites or low luminosity galaxies, we would expect evidence of dy-

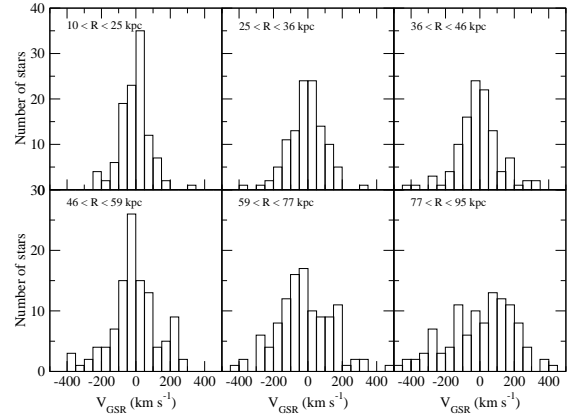


FIG. 8.— Histograms of the velocity distribution for 6 bins containing equal numbers of stars (the distance ranges sampled are indicated in figure legends). The two more distant bins appear to have a much less Gaussian distribution than the four bins at $R < 60$ kpc.

namical youth and tidal heating, as we observe in Fig. 4 and 5.

A possible alternative explanation is that the dark halo is very massive. Gnedin et al. (2010) has recently argued for a very massive halo based on the flatness of the velocity dispersion profile. However, in this case the mass to light ratio needed would exceed several hundred. Tidal heating may also produce an increasing velocity dispersion, as is observed in some dwarf galaxies (Munoz, Majewski & Johnston 2006). These explanations, while possible, would not probably produce the non Gaussian velocity dispersion observed at large radii.

The combined evidence from the space distribution and kinematics of BHB stars points to a very large and metal poor halo, whose outer regions appear to have been accreted relatively recently from low luminosity satellites, analogous to the copious tidal debris observed in M31. Although large streams are not observed the data appear to be in comparatively good agreement with theoretical predictions, although it is possible that minor mergers are more important than expected. More observations as well as models to truly ‘observe’ the simulated halos in the same fashion as the data and directly compare theory and reality will be needed to refine our understanding of the formation of the Milky Way.

We would like to thank the anonymous referee for a very helpful report which clarified many points in this paper. We thank the 2dF Quasar Survey for making their data available to the community and in particular Scott Croom for answering many questions on the data. We warmly thank all the present and former staff of the Anglo-Australian Observatory for their work in building and operating the 2dF and 6dF facilities. The 2QZ and 6QZ are based on observations made with the AAT and the UKST.

Facilities: AAT (2dF).

REFERENCES

- Battaglia G. et al. 2005, MNRAS, 365, 433
Beers, T. C., Rossi, S., O'Donoghue, D., Kilkenny, D., Stobie, R. S., Koen, C. & Wilhelm, R. 2001, MNRAS, 320, 451
Bell E. F. et al. 2008, ApJ, 680, 295
Belokurov V. et al. 2006, ApJ, 642, L137
Brown W. R., Geller M. J., Kenyon S. J. & Diaferio A. 2010, AJ, 139, 59
Carollo D. et al. 2007, Nature, 450, 1020
Carollo D. et al. 2009, astro-ph 0909.3109
Chapman S. C., Ibata R., Lewis G. F., Ferguson A. M. N., Irwin, M., McConnachie A. & Tanvir, N. 2006, ApJ, 653, 255
Cooper A. C. et al. 2009, astro-ph 0910.3211
Croom S. et al. 2004, MNRAS, 349, 1397
Dehnen W. & Binney J. 1998, MNRAS, 298, 387
Eggen O. J., Lynden-Bell D. & Sandage A. 1962, ApJ, 136, 748
Freeman K. & Bland-Hawthorn J. 2002, ARA&A, 40, 487
Gnedin, O., Brown, W. R., Geller, M. J. & Kenyon, S. J. 2010, astro-ph 1005.2619
Hambly N. C. et al. 2001, MNRAS, 326, 1279
Harris W. E., Harris, G. L. H., Layden A. C. & Wehner, E. M. H. 2007, ApJ, 666 903
Ibata R. A., Gilmore G. & Irwin M. J. 1994, Nature, 370, 194
Ibata R. A., Irwin M. J., Lewis G., Ferguson A. M. N. & Tanvir N. 2001, Nature, 412, 49
Ibata R. A. et al. 2007, ApJ, 671, 1591
Johnston K. V., Bullock J. S., Sharma S., Font A., Robertson B. E. & Leitner S. N. 2008, ApJ, 689, 936
Kalirai J. et al. 2006, ApJ, 648, 389
Kinman T. D., Cacciari C., Bragaglia A., Buzzoni A. & Spagna A. 2007, MNRAS, 375, 1381
Koch A. et al. 2008, ApJ, 689, 958
Layden A. C., Hanson R. B., Hawley S. L., Klemola A. R. & Hanley C. 1996, AJ, 112, 2110
Lewis I. et al. 2002, MNRAS, 333, 279
Lynden-Bell D. & Lynden-Bell R. 1995, MNRAS, 275, 429
Martinez-Delgado D. et al. 2010, astro-ph, 1003.4860
Majewski S. R., Skrutskie M. F., Weinberg M. D. & Ostheimer J. C. 2003, ApJ, 599, 1082
McConnachie A. W. et al. 2009, Nature, 461, 66
Morrison H. L., Mateo M., Olszewski E. W., Harding P., Dohm-Palmer R. C., Freeman K. C., Norris J. E. & Morita M. 2000, AJ, 119, 2254
Munari, U., Sordo, R., Castelli, F. & Zwitter, T. 2005, A&A, 442, 1127
Munoz R. R., Majewski S. R. & Johnston K. V. 2006, ApJ, 679, 346
Pier, J. 1983, ApJS, 53, 791
Robin A. C. et al. 2007, ApJS, 172, 545
Searle L. & Zinn R. J. 1978, ApJ, 225, 357
Sesar B. et al. 2010, ApJ, 708, 717
Smith M. C., Wyn Evans N. & Ahn J. H. 2009, ApJ, 698, 1110
Starkenburger E. et al. 2009, ApJ, 689, 567
van Hese, E., Baes, M. & Dejonghe, H. 2009, ApJ, 690, 1280
Walker M. G., Mateo M., Olszewski E. W., Bernstein R., Wang, X. & Woodroffe M. 2006, AJ, 131, 2114
Watkins L. L. et al. 2009, MNRAS, 398, 1757
Yanny B. M. et al. 2000, ApJ, 540, 825
Xue X. X. et al. 2008, ApJ, 648, 1143